



HAL
open science

The Fate of Shear-Oscillated Amorphous Solids

Chen Liu, Ezequiel E. Ferrero, Eduardo A. Jagla, Kirsten Martens, Alberto Rosso, Laurent Talon

► **To cite this version:**

Chen Liu, Ezequiel E. Ferrero, Eduardo A. Jagla, Kirsten Martens, Alberto Rosso, et al.. The Fate of Shear-Oscillated Amorphous Solids. 2021. hal-03349896

HAL Id: hal-03349896

<https://hal.science/hal-03349896>

Preprint submitted on 20 Sep 2021

HAL is a multi-disciplinary open access archive for the deposit and dissemination of scientific research documents, whether they are published or not. The documents may come from teaching and research institutions in France or abroad, or from public or private research centers.

L'archive ouverte pluridisciplinaire **HAL**, est destinée au dépôt et à la diffusion de documents scientifiques de niveau recherche, publiés ou non, émanant des établissements d'enseignement et de recherche français ou étrangers, des laboratoires publics ou privés.

The Fate of Shear-Oscillated Amorphous Solids

Chen Liu,¹ Ezequiel E. Ferrero,² Eduardo A. Jagla,³ Kirsten Martens,⁴ Alberto Rosso,⁵ and Laurent Talon⁶

¹*Laboratoire de Physique de l'Ecole Normale Supérieure, Paris, France*

²*Instituto de Nanociencia y Nanotecnología, CNEA-CONICET,*

Centro Atómico Bariloche, (R8402AGP) San Carlos de Bariloche, Río Negro, Argentina.

³*Centro Atómico Bariloche, Instituto Balseiro, Comisión Nacional de Energía Atómica, CNEA, CONICET, UNCUYO, Av. E. Bustillo 9500 R8402AGP S. C. de Bariloche, Río Negro, Argentina*

⁴*Univ. Grenoble Alpes, CNRS, LIPhy, 38000 Grenoble, France*

⁵*Université Paris-Saclay, LPTMS, CNRS, 91405 Orsay, France*

⁶*Université Paris-Saclay, FAST, CNRS, 91405 Orsay, France*

The behavior of shear-oscillated amorphous materials is studied using a coarse-grained model. Samples are prepared at different degrees of annealing and then subject to athermal and quasistatic oscillatory deformations at various fixed amplitudes. The steady-state reached after several oscillations is fully determined by the initial preparation and the oscillation amplitude, as seen from stroboscopic stress and energy measurements. Under small oscillations, poorly annealed materials display *shear-annealing*, while ultra-stabilized materials are insensitive to them. Yet, beyond a critical oscillation amplitude, both kind of materials display a *discontinuous* transition to the same *mixed* state composed by a fluid shear-band embedded in a marginal solid. Quantitative relations between uniform shear and the steady-state reached with this protocol are established. The transient regime characterizing the growth and the motion of the shear band is also studied.

Amorphous solids are a vast class of materials, common in nature and ubiquitous for human applications. Their mechanical behaviour is strongly affected by the preparation protocol: poorly annealed materials, such as emulsions, foams or gels, are soft and ductile, while well annealed materials such as metallic glasses, ceramics and silica are hard and brittle[1, 2]. Under a uniform deformation, the former tend to melt into a liquid, while the latter fail with a sharp stress-drop and the appearance of a thin liquid shear-band[3–5]. Although we tend to distinguish between these two kind of yielding, a debate is open: ductile materials could also display stress overshoots[5–8]. Beyond finite-size issues[6–8], dealing only with transient states does not help to settle the discussion. This is where an oscillatory deformation protocol[9–18] becomes handy, since it opens the possibility of characterizing a transition in terms of stationary states. In molecular dynamics (MD) simulations, two different “phases” have been identified: For moderate strain amplitudes Γ , the material appears solid and is progressively annealed[10, 11, 15–17] as oscillation cycles accumulate. Above a critical amplitude Γ_c , further shear-annealing is prevented and a shear-band coexists with a solid[10, 11, 16, 17, 19]. Despite a rapidly growing literature[9–27], basic questions remain to be addressed: (i) the nature of the transition at Γ_c , (ii) the relation between steady-states in the two protocols (oscillatory and uniform shear), and (iii) how those states are reached.

To answer these questions, in this Letter we use a coarse-grained approach, which goes beyond natural limitations of MD simulations. We find that the transition from solid to flow at Γ_c is discontinuous. We quantitatively relate properties of the emerging phases in oscillatory shear with those of the uniform-deformation protocol. Moreover, we describe transient stages previously unexplored. To do that, we prepare samples at differ-

ent degrees of annealing, characterized by the initial energy E_{init} per unit volume, and subject them to oscillatory deformations at various fixed amplitudes Γ until steady-states are reached. We find that once a *driving condition* (E_{init}, Γ) is chosen, it univocally defines the material’s fate in the steady-state; allowing us to fill a sort of *phase diagram*. Very well-annealed samples ($E_{\text{init}} < E^*$, with E^* a critical annealing level) are insensitive to small oscillations, while poorly-annealed samples ($E_{\text{init}} > E^*$) exhibit *shear-annealing* for large enough sub-critical Γ . We therefore distinguish between *stable solids*, that keep memory of their initial condition, and *marginal solids* which result from poorly-annealed samples losing memory of their initial conditions due to the shear-annealing by oscillations. Yet, when the oscillation amplitude reaches the critical threshold $\Gamma_c(E_{\text{init}})$, every sample undergoes a *discontinuous* transition, comprising a jump in stress and energy, towards *the same* mixed solid-fluid state. Part of the system melt in a shear-band while the rest becomes a critical solid of energy E^* , independently on the initial condition. The fluid in the band corresponds to the one of the stationary state at large uniform quasi-static shear and holds at most the uniform yield stress Σ_y . As Γ is further increased, the width of the shear-band scales as a power of $(\Gamma - \Sigma_y/\mathcal{G})$, with \mathcal{G} the effective shear-modulus, further relating uniform and oscillatory protocols. Also, a rich transient dynamics towards the steady-state above Γ_c is unveiled. We show a band-width growth as a function of the number of oscillation cycles that is reminiscent of critical domain coarsening. Surprisingly, once the band reaches its stable width it ballistically sweeps out the deeply-annealed regions, if present, turning them in the critical solid of energy E^* , and finally displays an (anomalous) diffusion. Overall, our Letter offers answers to fresh issues raised by MD simulations of glasses.

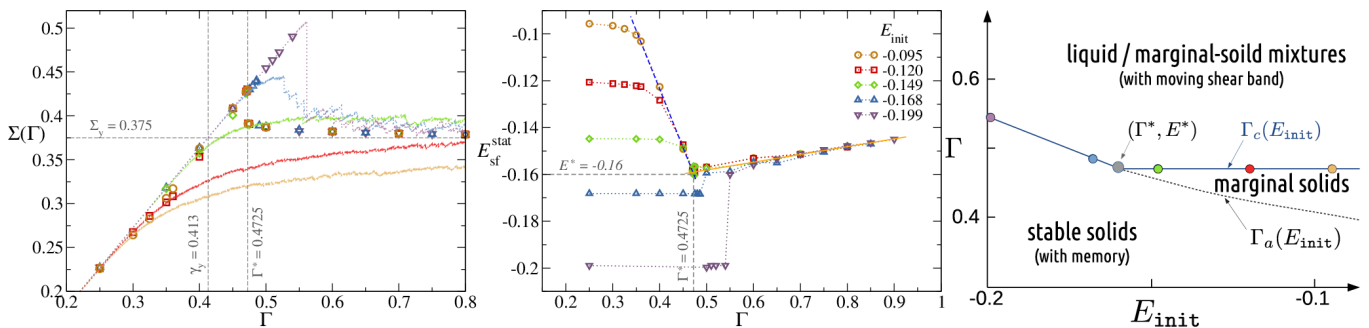


Figure 1. *Stationary properties*– (a) Symbols: Maximum stress $\Sigma(\Gamma)$ versus the oscillatory strain amplitude Γ . Curves: Stress-strain produced by quasi-static uniform shear. Different colors code for different degrees of initial annealing, signaled in (b). System size is 128^2 . (b) Stress-free steady energy $E_{\text{sf}}^{\text{stat}}$ versus the Γ . The purple dashed-line corresponds to “marginal solids”. The orange solid line displays a fit of $E_{\text{sf}}^{\text{stat}}(\Gamma)$ discussed in the text. (c) “Phase diagram” classifying driving conditions $(E_{\text{init}}, \Gamma)$ according to the steady-state they will reach: *stable solids* (strongly reminiscent of the initial state), *marginal solids* (shear-annealed solids independent of the initial condition), and *solid-liquid mixtures* characterized by an erratic shear-band. Color circles indicate Γ_c for different initial degrees of annealing E_{init} .

Methods – Our modelling is based on the evolution of a two-dimensional scalar strain field in a disordered potential, previously used to study yielding under uniform deformation[28–32]. Initial sample annealing is achieved by tuning the configuration of the disordered landscape (lower initial energies E_{init} for better annealed systems). Within this picture, the strain field behaves as a manifold propagating in a disorder medium[29, 30, 33]. Two essential ingredients are incorporated: the quadruple Eshelby’s elastic interaction[2, 34] and a disorder that rather than originating in quenched impurities mimics the random positions of particles. The local disorder changes irreversibly, even if the strain manifold revisits the same location. Details of our method are presented in the Supplemental Material (SM)[35].

Results – In view of their relevance in interpreting the shear oscillation results, we first reproduce some key features in uniform shear. In Fig.1(a) we show stress-strain curves for individual samples prepared at different degrees of annealing E_{init} (see also SM[35]). After an initial linear elastic response of slope $\mathcal{G} \approx 0.91$, all samples reach at large strain $\gamma \gtrsim 3$ a common plateau corresponding to the yield stress $\Sigma_y = 0.375 \pm 0.003$. The characteristic strain γ_y where plasticity becomes important is estimated as $\gamma_y = \Sigma_y/\mathcal{G} \simeq 0.413$. Poorly annealed materials display a monotonic crossover from an elastic solid to a liquid crossing γ_y , while well annealed systems remain elastic above γ_y up to a failure strain γ_f where a sharp stress downfall occurs. The overshoot gets larger for better annealed samples[3–5, 8]. In general, the total energy per volume of the material can be decomposed into two contributions: $E_{\text{tot}} = E_{\text{sf}} + \Sigma^2/(4\mu)$, where the second contribution is due to macroscopic elastic deformation (with $\mu = 1/2$ the shear modulus) and E_{sf} , called ‘stress-free energy’ afterward, characterizes the state of the material with zero macroscopic stress. In the large uniform shear limit $\gamma \rightarrow \infty$, where the memory of the initial state is completely erased, all samples

converge to a homogeneous stationary liquid state with $E_{\text{sf}}^{\text{stat}} = -0.122 \pm 0.001 \equiv E_{\text{liq}}$ (see SM[35] for details).

Now, in our oscillatory protocol, the material is deformed by quasi-statically varying the strain from 0 to Γ , then to $-\Gamma$ and subsequently back to 0 to complete one cycle of amplitude Γ . This cycle is repeated until a steady-state is reached. By varying Γ and E_{init} , we obtain an assortment of stationary states. Figure 1(a) shows the steady-state maximum stress[10, 15, 19] $\Sigma(\Gamma)$ as a function of Γ in comparison with uniform-shear load curves. Consistent with MD results, all samples exhibit a sharp jump of $\Sigma(\Gamma)$ at a critical strain amplitude $\Gamma_c(E_{\text{init}})$. The moderately annealed samples ($E_{\text{init}} = -0.095, -0.12$ and -0.149) fail at the same $\Gamma_c \approx 0.4725 \equiv \Gamma^*$, independently on the initial degree of annealing; while the more annealed samples ($E_{\text{init}} = -0.168$ and -0.199) experience a later failure at $\Gamma_c(E_{\text{init}}) \approx \gamma_f(E_{\text{init}}) > \Gamma^*$, stronger as better annealed is the sample. Once above Γ_c , the steady-state stress $\Sigma(\Gamma > \Gamma_c)$ for any initial state, is well identified with Σ_y of a stationary flowing state in the quasi-static uniform shear deformation. Figure 1(b) displays the stationary stress-free energy $E_{\text{sf}}^{\text{stat}}$ as a function of Γ [36]. For very small Γ , the stationary state $E_{\text{sf}}^{\text{stat}}$ strongly depends on E_{init} . Increasing Γ within the solid phase ($\Gamma < \Gamma_c$), two scenarios separated by a critical annealing $E^* \approx -0.16$ are observed. Samples with $E_{\text{init}} < E^*$ keep a perfect memory of their initial states up to melting, evidenced by $E_{\text{sf}}^{\text{stat}}(\Gamma) = E_{\text{init}}$ for all $\Gamma < \Gamma_c(E_{\text{init}})$ [15, 25]. Yet, for $E_{\text{init}} > E^*$ the phenomenology is richer: Increasing Γ , at some point, the stationary-state $E_{\text{sf}}^{\text{stat}}$ starts to decrease with the amplitude, losing memory of the initial condition. This is a manifestation of shear-annealing in the steady-state, as similarly observed in[10, 15, 25–27]. Notice that, for initially weakly annealed systems, there exist also a *transient* process of shear-annealing (described later on), where samples reach a lower-energy steady-state by oscillating at a fixed Γ . $E_{\text{sf}}^{\text{stat}}$ for $E_{\text{init}} > E^*$

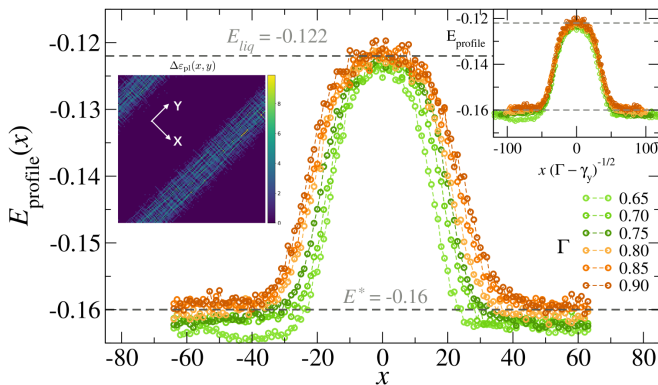


Figure 2. Energy profiles averaged along the y -axis for different Γ . $x = 0$ is set to the maximum location. *Left inset*: map of strain field during a half-cycle in the steady-state. *Right inset*: profiles collapse using $w_s(\Gamma) = a(\Gamma - \Gamma_0)^\alpha$ with $\Gamma_0 = \gamma_y = 0.413$ and $\alpha = 1/2$.

ends up collapsing to a common curve (purple dashed line in Fig. 1(b)), where the initial condition becomes irrelevant and $E_{\text{sf}}^{\text{stat}}$ depends only on Γ . We call “marginal solids” the stationary states lying on the purple dashed line, which terminates at Γ^* at the critical energy E^* . Once $\Gamma > \Gamma_c(E_{\text{init}})$, both $\Sigma(\Gamma)$ and $E_{\text{sf}}^{\text{stat}}(\Gamma)$ fall onto a unique curve, independent on E_{init} . The system develops a permanent liquid shear-band embedded in a solid phase, and the steady-state energy $E_{\text{sf}}^{\text{stat}}$ increases with Γ (Fig. 1(b)), see also [15, 19, 26]. From the previous discussion, we can associate to each E_{init} an amplitude $\Gamma_a(E_{\text{init}})$ above which the steady-state $E_{\text{sf}}^{\text{stat}}(\Gamma, E_{\text{init}})$ is independent on the initial annealing E_{init} .

As summarized in a diagram Fig.1(c), $\Gamma_a(E_{\text{init}})$ (dashed line) identifies with $\Gamma_c(E_{\text{init}})$ (solid line) below E^* , and bifurcates above it. The solid steady-states resulting from driving conditions below $\Gamma_a(E_{\text{init}})$ are strongly reminiscent of the initial state and called “stable solids”. In contrast, those driving conditions in between Γ_c and Γ_a correspond to solids that forget their initial condition and end up being “marginal solids” in the steady-state. Driving conditions in the region above $\Gamma_c(E_{\text{init}})$ lead to a steady-state mixed phase composed by a fluid shear band surrounded by a critical marginal solid, which we detail in the following.

Fig. 2 shows the averaged stress-free energy profile across a section orthogonal to the shear-band (evidenced in the strain field in the left-inset). The energy profile characterizes the band by a bell-shape. The interior of the band (top of the bell) has the same energy as the stationary liquid in uniform shear deformation $E_{\text{liq}} \approx -0.122$. The width w_s of the band increases with Γ and is well fitted by $w_s(\Gamma) = a(\Gamma - \Gamma_0)^\alpha$. A good collapse is found when rescaling the profiles with $\alpha = 1/2$ (right-inset of Fig. 2), reminiscent of the transient band dynamics in uniform shear [37]. We further notice two peculiarities: First, from the fit, Γ_0 identifies with γ_y instead of Γ^* , implying that at the transition,

the shear-band has a finite width $w_s(\Gamma^*) > 0$ (because $\gamma_y < \Gamma^*$). Second, the energy profile is independent on E_{init} and the energy at the bottom of the bell-shape coincides with the critical solid energy E^* . This allows to conclude that the mixture phase is completely independent on the initial degree of annealing and uniquely characterized by the width w_s : the stationary regime is composed of a fraction of critical solid at energy E^* and a shear-band made of the liquid of energy E_{liq} . Since $E_{\text{liq}} > E^*$, the monotonic growth of $E_{\text{sf}}^{\text{stat}}$ (Fig. 1(b)) can be rationalized in terms of the shear-band widening with Γ : $E_{\text{sf}}^{\text{stat}} \simeq E^* + (E_{\text{liq}} - E^*) \frac{a(\Gamma - \gamma_y)^\alpha}{L}$. This is tested in Fig. 1(b). It also implies that a discontinuity of $E_{\text{sf}}^{\text{stat}}$ at the transition $\Gamma_c = \Gamma^*$, even though small, is expected [10, 15, 25–27]. In addition, we observed that w_s is proportional to the linear system size, as also seen in the fact that $E_{\text{sf}}^{\text{stat}}$ shows no size dependence [35].

We now discuss the transient oscillatory dynamics. Figs.3(a-b) show the evolution of $E_{\text{sf}}(n)$, as the oscillation cycles n accumulate, for different driving conditions $(E_{\text{init}}, \Gamma)$. Below Γ_c (Fig.3(a)), ultra-stable systems ($E_{\text{init}} < E^*$) are unperturbed by the oscillations, while systems with $E_{\text{init}} > E^*$ shear-anneals if the amplitude is large enough. At amplitudes above $\Gamma_a(E_{\text{init}})$ all initial conditions are shear-annealed to the same stationary state, as observed for our three softest samples in Fig. 3(a). Above Γ_c (Fig.3(b)), all samples go to the same stationary state at large n . Our observations for the number n_T of cycles to reach steady-states are compatible with a divergence when approaching Γ_c reported in previous works [10, 13, 14, 16, 19]. Data for $(\Gamma < \Gamma_c)$ is shown in SM [35]. We switch now to the observation of different dynamical regimes for the mixed phase. For poorly annealed samples, the onset of the shear-band and its stabilization in a stationary width $w_s(\Gamma)$ occurs gradually and rapidly as the solid region shear-anneals to the critical state in a small number of cycles. Then the shear band diffuses in the material (see Fig. 4(a) and Video 1 [35]) with a mobility that increases with Γ . In well annealed systems instead, the transient is richer and we identify three dynamical regimes (Fig. 4(b), see also Video 2 [35]): (i) *Shear band formation and growth*. The initial band growth is observed at the top of Fig. 4(b) (see [35] for details). This initial coarsening of the shear-band is studied in Fig. 3(c) at different Γ . In all cases, the band width grows as $\sim n^{1/3}$ until reaching the stationary width $w_s \sim (\Gamma - \gamma_y)^{1/2}$. (ii) *Melting of the solid*. The now fully-formed shear band displays a ballistic motion preferentially invading the deeply annealed solid and leaving behind the critical solid of energy E^* . (iii) *Shear band diffusion*. When the shear-band has visited the entire system, all the regions outside the band have been modified into the critical marginal solid. The stationary state is reached and the band diffuses forever, maintaining its characteristic Γ -dependent width.

Discussion – Our mesoscopic model allows to recover the phenomenology of the oscillatory shear of amorphous materials reported by MD simulations [3, 10, 15, 25, 27]

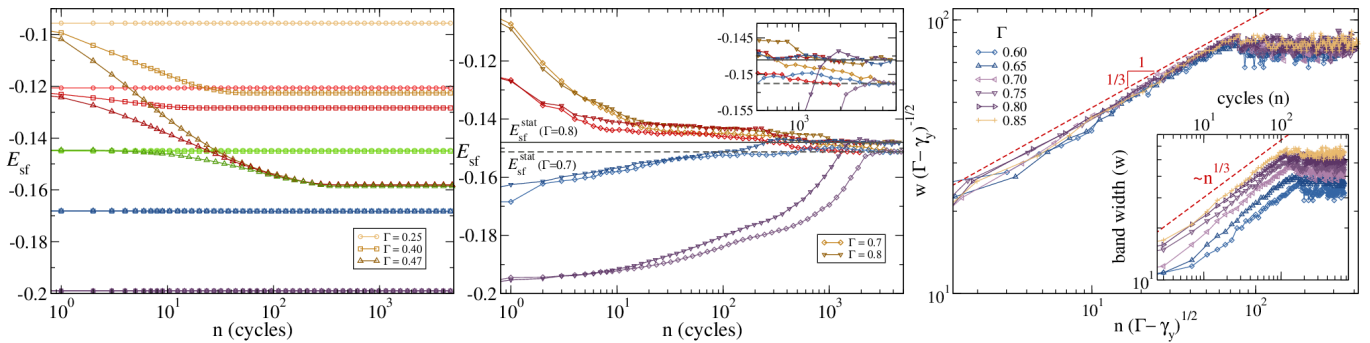


Figure 3. *Transient properties*– (a-b) Evolution of stress-free energy E_{sf} as the number of cycles n increases, for different amplitudes. Colors coding for different E_{init} are the same as in Fig.1. System size is 128^2 . (a) Solid phase ($\Gamma < \Gamma_c$). (b) Mixed phase ($\Gamma > \Gamma_c$). Inset in (b) shows a zoom-in to appreciate the difference in E_{sf}^{stat} for different Γ . (c) Shear-band width w as a function of n for different Γ . The initial condition is a well annealed solid ($E_{init} = -0.168$). The inset shows raw-data and the main panel the scaling $w(\Gamma - \gamma_y)^{-1/2}$ vs. $n(\Gamma - \gamma_y)^{1/2}$. The red dashed line is a power-law $\sim n^{1/3}$. System size is 256^2 .

and go beyond. While some emerging features can be already captured by even further simplified toy models as seen recently[13], keeping an spatial extent for the system and its geometry gives access to the full picture. We are able to univocally classify the oscillatory stationary states according to a “phase diagram” in the space of oscillation amplitude Γ and initial annealing level E_{init} , and relate them with the steady-states of the uniform-deformation protocol. Interestingly, the oscillatory protocol always shows a discontinuous transition in both stress and energy at a critical strain amplitude Γ_c , even in the case of ductile materials that melt homogeneously under uniform deformation. Notably, ductile materials mechanically anneal and harden at sub-critical amplitudes under oscillatory shear. Independently on the initial state, every system sheared at large amplitudes ends up in a steady-state displaying a permanent shear-band. This band contains a stationary fluid identical to the one obtained at large uniform deformations and is embedded in a solid matrix

which is not at all arbitrary. The solid surrounding the shear-band in this mixed phase is the critical marginal solid that has the energy of the critical annealing level E^* . A line of *amnesia* $\Gamma_a(E_{init})$ discriminate driving conditions (E_{init}, Γ) between *stable solids* and solids that shear-anneal and evolve towards a marginal line in the steady-state. Our approach gives also transparent access to the transient regimes of shear-band formation, growth and motion. For deeply-annealed samples, a small but finite width band first spreads the system, then grows with a power-law $\propto n^{1/3}$ of the number of oscillation cycles. Ulteriorly, the band invades ballistically the deeply-annealed solid, leaving behind the critical solid of energy E^* . Finally, it diffuses anomalously over all the system.

These results shed light to clarify some previous observations in the literature and open interesting directions of new research. One could ask, for example, whether the emergence of a transient state of multiple shear-bands is possible in the large system limit, and how do they merge in a single band in the steady-state (or not). Also, to which extent the incorporation of “reversible” plastic events observed in atomistic simulations[16–20, 23, 24] enriches the overall phenomenology. Those are absent in our present model by choice, but easy to include by locally quenching the disordered potential [14]. Further, the critical annealing E^* detected in the oscillatory protocol could play also a relevant role in uniform shear, where the ductile-brittle yielding transition is a matter of vivid discussion[3, 5, 8]. It is indeed suggestive that the load curve of our closest to E^* sample sits near to the apparent transition between ductile/brittle yielding probed by the uniform shear curves. More importantly, it will be interesting to test experimentally these predictions, with new measurements closer to the quasi-static limit, since in the standard setups the oscillations are relatively fast and the material softens instead of annealing and hardening. In general, we hope that our results will motivate new research directions in the study of low temperature amorphous materials, from realistic large-scale

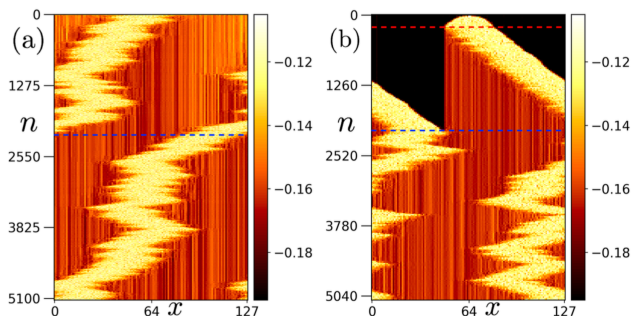


Figure 4. Energy profiles $E_{profile}(x)$ evolving as function of the number n of oscillation cycles for $\Gamma = 0.7$. Light colors represent higher energies and evidence the position of the shear-band. (a) A poorly annealed sample with $E_{init} \approx -0.12$. (b) Well annealed sample with $E_{init} \approx -0.199$. The red dashed-line in (b) indicates the stabilization of the band width at $n \approx 220$. When the blue dashed-line is reached, the band has visited the entire system.

atomistic simulations to experiments.

ACKNOWLEDGMENTS

We are indebted to M. Ozawa for illuminating discussions on the subject. We thank S. Sastry for kind feed-

back on an earlier version of this manuscript. EEF acknowledges support from PICT-2017-1202. Authors acknowledge support from the collaboration project ECOS Sud-MINCYT A16E01. CL, AR and LT acknowledges support by “Investissement d’Avenir” LabEx PALM (Grant No. ANR-10-LABX-0039-PALM)

-
- [1] D. Bonn, M. M. Denn, L. Berthier, T. Divoux, and S. Manneville, Yield stress materials in soft condensed matter, *Rev. Mod. Phys.* **89**, 035005 (2017-08).
- [2] A. Nicolas, E. E. Ferrero, K. Martens, and J.-L. Barrat, Deformation and flow of amorphous solids: Insights from elastoplastic models, *Rev. Mod. Phys.* **90**, 045006 (2018-12).
- [3] M. Ozawa, L. Berthier, G. Biroli, A. Rosso, and G. Tarjus, Random critical point separates brittle and ductile yielding transitions in amorphous materials, *Proceedings of the National Academy of Sciences* **115**, 6656 (2018).
- [4] M. Popović, T. W. J. de Geus, and M. Wyart, Elastoplastic description of sudden failure in athermal amorphous materials during quasistatic loading, *Phys. Rev. E* **98**, 040901 (2018).
- [5] H. J. Barlow, J. O. Cochran, and S. M. Fielding, Ductile and brittle yielding in thermal and athermal amorphous materials, *Phys. Rev. Lett.* **125**, 168003 (2020).
- [6] M. Ozawa, L. Berthier, G. Biroli, and G. Tarjus, Rare events and disorder control the brittle yielding of amorphous solids (2021), [arXiv:2102.05846 \[cond-mat.soft\]](https://arxiv.org/abs/2102.05846).
- [7] R. David, R. Corrado, and L. Edan, Finite-size study of the athermal quasistatic yielding transition in structural glasses (2021), [arXiv:2104.02441 \[cond-mat.soft\]](https://arxiv.org/abs/2104.02441).
- [8] S. M. Fielding, Yielding, shear banding and brittle failure of amorphous materials, [arXiv preprint arXiv:2103.06782](https://arxiv.org/abs/2103.06782) (2021).
- [9] D. Fiocco, G. Foffi, and S. Sastry, Encoding of memory in sheared amorphous solids, *Phys. Rev. Lett.* **112**, 025702 (2014).
- [10] P. Leishangthem, A. D. S. Parmar, and S. Sastry, The yielding transition in amorphous solids under oscillatory shear deformation, *Nature Communications* **8**, 14653 EP (2017).
- [11] P. Das, A. D. S. Parmar, and S. Sastry, Annealing glasses by cyclic shear deformation (2020), [arXiv:1805.12476 \[cond-mat.soft\]](https://arxiv.org/abs/1805.12476).
- [12] D. Hexner, A. J. Liu, and S. R. Nagel, Periodic training of creeping solids, *Proceedings of the National Academy of Sciences* **117**, 31690 (2020).
- [13] S. Sastry, Models for the yielding behaviour of amorphous solids (2020), [arXiv:2012.06726 \[cond-mat.soft\]](https://arxiv.org/abs/2012.06726).
- [14] K. Khirallah, B. Tyukodi, D. Vandembroucq, and C. E. Maloney, Yielding in an integer automaton model for amorphous solids under cyclic shear, *Phys. Rev. Lett.* **126**, 218005 (2021).
- [15] W.-T. Yeh, M. Ozawa, K. Miyazaki, T. Kawasaki, and L. Berthier, Glass stability changes the nature of yielding under oscillatory shear, *Phys. Rev. Lett.* **124**, 225502 (2020).
- [16] T. Kawasaki and L. Berthier, Macroscopic yielding in jammed solids is accompanied by a nonequilibrium first-order transition in particle trajectories, *Physical Review E* **94**, 022615 (2016).
- [17] I. Regev, T. Lookman, and C. Reichhardt, Onset of irreversibility and chaos in amorphous solids under periodic shear, *Phys. Rev. E* **88**, 062401 (2013).
- [18] I. Regev, J. Weber, C. Reichhardt, K. A. Dahmen, and T. Lookman, Reversibility and criticality in amorphous solids, *Nature Communications* **6**, 8805 EP (2015).
- [19] D. Fiocco, G. Foffi, and S. Sastry, Oscillatory athermal quasistatic deformation of a model glass, *Phys. Rev. E* **88**, 020301 (2013).
- [20] N. V. Priezjev, Reversible plastic events during oscillatory deformation of amorphous solids, *Phys. Rev. E* **93**, 013001 (2016).
- [21] N. V. Priezjev, Collective nonaffine displacements in amorphous materials during large-amplitude oscillatory shear, *Phys. Rev. E* **95**, 023002 (2017).
- [22] I. Regev and T. Lookman, The irreversibility transition in amorphous solids under periodic shear, in *Avalanches in Functional Materials and Geophysics* (Springer, 2017) pp. 227–259.
- [23] I. Regev and T. Lookman, Critical diffusivity in the reversibility–irreversibility transition of amorphous solids under oscillatory shear, *Journal of Physics: Condensed Matter* **31**, 045101 (2018).
- [24] M. Mungan, S. Sastry, K. Dahmen, and I. Regev, Networks and hierarchies: How amorphous materials learn to remember, *Phys. Rev. Lett.* **123**, 178002 (2019).
- [25] H. Bhaumik, G. Foffi, and S. Sastry, The role of annealing in determining the yielding behavior of glasses under cyclic shear deformation (2019), [arXiv:1911.12957 \[cond-mat.dis-nn\]](https://arxiv.org/abs/1911.12957).
- [26] A. D. S. Parmar, S. Kumar, and S. Sastry, Strain localization above the yielding point in cyclically deformed glasses, *Phys. Rev. X* **9**, 021018 (2019).
- [27] P. Das, H. Vinutha, and S. Sastry, Unified phase diagram of reversible–irreversible, jamming, and yielding transitions in cyclically sheared soft-sphere packings, *Proceedings of the National Academy of Sciences* **117**, 10203 (2020).
- [28] E. A. Jagla, Strain localization driven by structural relaxation in sheared amorphous solids, *Phys. Rev. E* **76**, 046119 (2007).
- [29] I. Fernández Aguirre and E. A. Jagla, Critical exponents of the yielding transition of amorphous solids, *Phys. Rev. E* **98**, 013002 (2018-07).
- [30] E. E. Ferrero and E. A. Jagla, Elastic interfaces on disordered substrates: From mean-field depinning to yielding, *Phys. Rev. Lett.* **123**, 218002 (2019-11).
- [31] E. A. Jagla, Tensorial description of the plasticity of amorphous composites, *Phys. Rev. E* **101**, 043004 (2020).
- [32] E. E. Ferrero and E. A. Jagla, Properties of the density of

- shear transformations in driven amorphous solids, *Journal of Physics: Condensed Matter* **33**, 124001 (2021).
- [33] J. Lin, E. Lerner, A. Rosso, and M. Wyart, Scaling description of the yielding transition in soft amorphous solids at zero temperature, *Proceedings of the National Academy of Sciences* **111**, 14382 (2014).
- [34] J. Eshelby, The Determination of the Elastic Field of an Ellipsoidal Inclusion, and Related Problems, *Proceedings of the Royal Society A: Mathematical, Physical and Engineering Sciences* **241**, 376 (1957).
- [35] See Supplemental Material at [URL will be inserted by publisher], which also includes references...
- [36] E_{sf} characterizes the intrinsic state without external load, while the stroboscopic energy [10, 26, 27] incorporates an arbitrary elastic contribution when $\Gamma > \Gamma_c$.
- [37] E. Jagla, Shear band dynamics from a mesoscopic modeling of plasticity, *Journal of Statistical Mechanics: Theory and Experiment* **2010**, P12025 (2010).